PAPER 67 – EXPERIMENTAL STUDY OF THE PRESSURE DROP AND FLOODING IN A ROTATING PACKED BED

Usman Garba[1,2] , David Rouzineau[1] , Michel Meyer[1]

[1]Chemical Engineering Laboratory, University of Toulouse, CNRS, INPT, UPS, Toulouse, France
[2]Usmanu Danfodiyo University Sokoto, Nigeria
[*]Email: usman.garba@udusok.edu.ng

ABSTRACT
Embedded processes require compactness, low energy consumption, and insensitivity to gravity. Centrifugal processes respond to the last characteristic. Centrifugal force is used instead of the gravitational force with almost zero sensitivity to variations in the gravitational force. We studied a rotating packed bed (RPB) as a gas/liquid contactor for absorption. We focused our attention on the hydrodynamic behavior of this device. Previous studies on RPB flooding and operating limits dwelled on virtual observations and pressure drop variations. However, physical visualizations are subjective because RPB pressure drop variations are too inconsistent to be used to determine the upper operating limit during RPB operations. A robust quantitative method of obtaining RPB flooding limits based on the flow rate of the ejected liquid, supported by visual observation and pressure drop measurement, was presented. The aim was to identify, with greater accuracy, RPB hydrodynamic characteristics and provide a more standard method of identifying same.

KEYWORDS: Rotating packed bed, pressure drop, Flooding, Gas/liquid contactor, hydrodynamics,

1. INTRODUCTION

Reliance on gravitational force makes conventional packed columns for separation processes such as distillation and absorption to have unimpressive sizes and physical footprints which makes them uneconomical, especially where space and weight are (Adekola et al., 2012; Hilpert & Repke, 2021). The operating ranges of non-rotating, conventional, packed bed columns (PBCs) are limited by gravitational and frictional forces acting in opposite directions on the down-flowing liquid and the gas flowing from the bottom of the column. A RPB, also called HIGEE (High g) contactor, is a compact process intensification equipment in which a combination of sizeable allowable gas and liquid flowrates is achieved by superimposing gravitational force with centrifugal force. In RPBs, the higher gravitational force factor employable raises the combined operating range of the throughputs in addition to their flexibility due to the additional degree of freedom offered by the rotation speed (Groß et al., 2018).

A fundamental aspect of the modeling, design, optimization, and implementation of pilot-scale and subsequent scale-up of RPBs is the clear understanding of the principles of its hydrodynamics via accurate prediction of the pressure drops and upper operating limits (Hendry et al., 2020; Neumann, et al., 2017a). Also, (Zhang et al., 2020) observed that the mass transfer performance and efficiency of an RPB, as reflected by its gas pressure drop, is closely linked to its hydrodynamic characteristics, operating costs, and energy requirements. Hydrodynamic characteristics such as the pressure drop of an RPB are a useful index in measuring its resistance and consequent energy consumption (Liu et al., 2018). Many studies were carried out to evaluate the influence of pressure drop in many RPB operations with empirical and semi-empirical models established (Jiao et al., 2010; Singh et al., 1992). RPB hydrodynamic parameters extensively reported in the literature include liquid holdup (Burns et al., 2000; Burns & Ramshaw, 1996), gas pressure drop (Neumann et al., 2017b; Pyka et al., 2022), liquid dispersion (Burns & Ramshaw, 1996; Xie, 2019) and, flooding (Hendry et al., 2020; Lockett, 1995). Although extensive research has been conducted and documented using RPBs, with many of its applications explored at the industrial scale, its design approach is still case-specific. It thus requires improvements (Neumann, et al., 2017a).

This work presents a robust quantitative method of obtaining RPB upper operating limit based on the flow rate of the ejected liquid, supported by visual observation and pressure drop measurements. This was achieved by connecting a hydrocyclone to the gas outlet. In addition, a comprehensive pressure drop behavior and flooding for a countercurrent water-air system and a single-block stainless steel wire mesh packing using a double jet nozzle for the liquid inlet

were used to study the hydrodynamics of the pilot-scale RPB. The aim was to improve further the understanding of RPB hydrodynamics for design, scale-up, and energy conservation purposes.

The relatively high rotation speeds of RPBs combined with the size of the equipment make it possible to implement forces more than 100 times greater than gravity, greatly intensifying the transfer phenomena between phases (Pan et al., 2017). Rapid contact surface replacement in RPBs allows for high effective surface area packings of 2000 to 5000m^2/m^3 (Pan et al., 2017). This allows for higher mass transfer characteristics: gas-liquid interfacial area, gas-side and liquid-side volumetric mass transfer coefficients, and height of transfer unit (Cheng & Tan, 2011; Zhang et al., 2011). Also, this allows for the same separation performance in RPB to have much more flexible and compact equipment with a wider operating range than a gravity column used for absorption (L. L. Zhang et al., 2011). Overall, compared to conventional gravity columns, for a comparable processing capacity and efficiency, a RPB offers rotation as an extra degree of freedom, serves as the foundation of modular plants, and is more miniaturized with higher flexibility and energy efficiency (Neumann et al., 2018). The characteristics mentioned above make RPBs emblematic equipment for process intensification. Consequently, RPBs have been employed for various purposes in diverse fields such as separation processes, synthesis, and preparation of micro and nano-particles, petroleum products processing, biodiesel production, medical sciences, and pollution control (Hilpert & Repke, 2021; Neumann et al., 2018; L. L. Zhang et al., 2011).

A conventional, single-stage RPB is shown in Figure 1. It comprises of a casing surrounding a rotor mounted on a shaft and rotated by a motor. The rotor is a motor-driven, ring-shaped cylinder that encloses an annular packing mounted on either a horizontal or a vertical shaft. In countercurrent operation mode, gas is introduced into the outer periphery of the packing from the casing. The liquid is usually introduced into the center (or "eye") of the rotor via the liquid inlet through a stationary set of nozzles (liquid distributor) into the packing from the top of the RPB. After its transformation by centrifugal shear forces, the liquid flows in the form of rivulets, droplets, or films as determined by the rotation speed (Burns et al., 2000). The casing wall finally collects it and flows downwards under gravity, leaving the casing via the liquid outlet.

As equipment for efficient multi-phase mixing and mass transfer, (Yuan et al., 2022) identified RPB packing as its core component. Because of its excellent mass transfer characteristics, stainless steel wire mesh is commonly used as RPB packing (Chen et al., 2006). Conventional packed beds have constant cross-sections. Thus, their packing pores are nearly wholly filled throughout the column during flooding, causing a noticeable, steep rise in pressure drop.

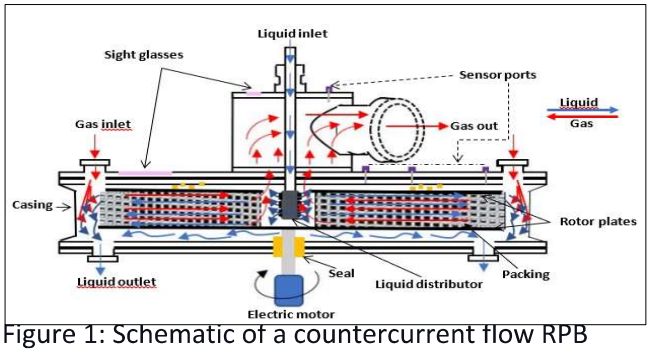

Figure 1: Schematic of a countercurrent flow RPB

However, due to the rotor geometry, RPB packings have variable cross-sections. The centrifugal forces are lowest at the center (eye) of the rotor. Hence, RPB flooding occurs in the eye from where the liquid is ejected. Consequently, pressure drop variations during flooding in RPBs are not consistent as the sole indicator of flooding. (Neumann et al., 2017a), and Lockett (Lockett, 1995) also reported that in contrast to conventional columns, for RPBs, no sharp inflection in the total pressure drop or the holdup of the liquid with the gas velocity was observed during flooding. The procedure for visually determining the upper operating limit is to neutralize two operating variables and manipulate the third one (Groß et al., 2018). Therefore, it is possible to carry out two procedures to reconfirm the results. The speed of the rotor and the liquid flow rate may be set to a constant value then the gas flow rate gradually increases until an excessive splash of the liquid is observed in the eye of the rotor. Allowing the gas flow rate to increase beyond the upper operating limit will cause the liquid to accumulate in the eye of the rotor. (Groß et al., 2018;

Neumann et al., 2017b) recommended the use of a combination of visual and quantitative approaches to adequately study the flow behavior in RPBs, while (Groß et al., 2018) observed that due to observed inconsistencies, the use of physical and visual observations and the measurement of pressure drop variations alone are not sufficiently adequate to predict flooding behavior in RPBs. (Burns et al., 2000) used liquid holdup, while (Hendry et al., 2020) measured the flow rate of entrained liquid from the eye of the rotor to identify the upper operating limits in RPBs.

2. MATERIALS AND METHODS/METHODOLOGY/EXPERIMENTAL PROCEDURE

The experimental setup is shown in Figure 2. The RPB was a pilot-scale RPB 500 from ProCeller® located at the Laboratoire de Génie Chimique (LGC) in Toulouse (France). The RPB was a single-stage, vertical rotor type with a casing diameter of 0.676m, an inner rotor diameter of 0.160m, and an outer rotor diameter of 0.500m. The packing was a conventional, multi-layered, single-block, stainless steel wire mesh with an axial height of 0.040m, a specific surface of 2400 m^2/m^3, and a porosity of 86%. Visual observation was possible using two inspection glasses placed directly above the eye of the rotor and another on the casing (Figure 3a). To aid the systematic collection and subsequent measurement of ejected water from the eye of the rotor during flooding, a hydrocyclone was connected to the gas outlet. A countercurrent air-water system was used for all the experiments. The rotation speed of the rotor was selected and auto-controlled via a variable frequency drive. The liquid was pumped to the RPB using a peristaltic pump and controlled with a valve. The liquid flow rate was measured with a panel-type rotameter and sprayed from the center of the RPB using a dual nozzle, flat fan liquid distributor. The liquid was recirculated to the feed tank using a bypass line. An air supply from the general laboratory compressor was used. The gas was introduced into the outside of the RPB into the casing through twin gas inlets and leaves after passing through the packing via the gas outlet. While the liquid sprays outwards from the center of the packing to its periphery. A pressure sensor connected to a pressure transmitter was placed across the two points to measure the pressure drop between the packing periphery and the gas outlet. Pressure drop was measured in real time by interfacing the sensor to a computer using a data acquisition system.

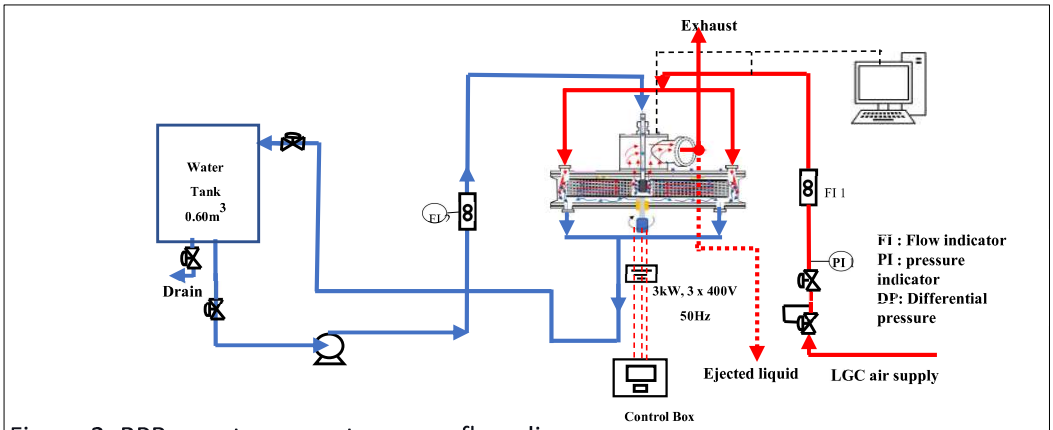

Figure 2: RPB countercurrent process flow diagram

The range of operating parameters studied was: gas flow rate (V_G), 0-400Nm^3/h; liquid flow rate (V_L), 0-0.75m^3/h and rotation speed 0-1500 revolutions per minute (RPM). Each experimental run was for 5 minutes. In the dry pressure drop measurements, the frictional pressure drop was first measured by passing air at 100Nm^3/h through the stationary rotor and then measuring the pressure drop. The experiment was repeated by increasing the airflow rate in steps of 50Nm^3/h. The same procedure was repeated with the rotor at various rotation speeds. Next, the effect of the rotation speed was investigated, initially via the centrifugal pressure drop. Without liquid and gas flow, the rotor was set to an initial speed of 100 rpm. The rotation speed was subsequently changed stepwise. The effect of rotation speed was further investigated by varying the rotation speed at constant gas flow rates. For the wet pressure drop, rotation speeds and liquid flow rates were kept while the gas flow rate was increased stepwise. This was followed by another set of experiments during which the gas flow rate and rotation speed were kept constant while the liquid flow rate was increased. The liquid flow rate and rotation speed were kept constant to determine the upper operating limit. In contrast, the gas flow rate was increased stepwise until the first drops of water were observed from the gas outlet according to the arrangement shown in Figure 3e. This point was taken as the upper operating limit of the RPB at the prevailing combination of operating factors. The reduction in rotation speed was continued gradually, with the amount

of ejected water measured at each step after attaining a steady state of operation. Flooding points of the RPB operations were determined by visual observation of excessive water splashing at the RPB eye, with or without a sharp increase in pressure drop. The volume of water ejected at each step change of the gas flowrate was collected and measured using a measuring cylinder, and the flooding point was taken following the recommendation of (Hendry et al., 2020) when,

$$flowrate\ of\ ejected\ liquid \geq 8\%\ liquid\ flowrate \quad (1)$$

3. RESULTS AND DISCUSSION

Figure 4(a) shows that dry pressure drop increases with increased rotor speed. A slow increase in pressure drop was obtained at low rotational speeds from 100 to 550 RPM. Above 600 RPM, a rapid and almost linear increase in pressure drop was obtained. This phenomenon may be due to the greater need to overcome the pressure drop caused by rotation (centrifugal head) at higher rotational speeds, which consequently causes the air in the rotor and between it and the casing to rotate. The dry bed average increase in pressure drop per unit increase in rotation speed in the range investigated was 0.75Pa/rpm. This shows that centrifugal pressure contributes significantly to the total dry-packing pressure drop. Figure 4(b) also shows a substantially linear increase in pressure drop with increasing gas flow rate. The effects of gas inertia and friction primarily cause this. On average, Figure 4(b) shows that the average increase in pressure drop per unit increase in gas flow rate was 4.11Pa/Nm^{3}h^{-1} within the operating range investigated.

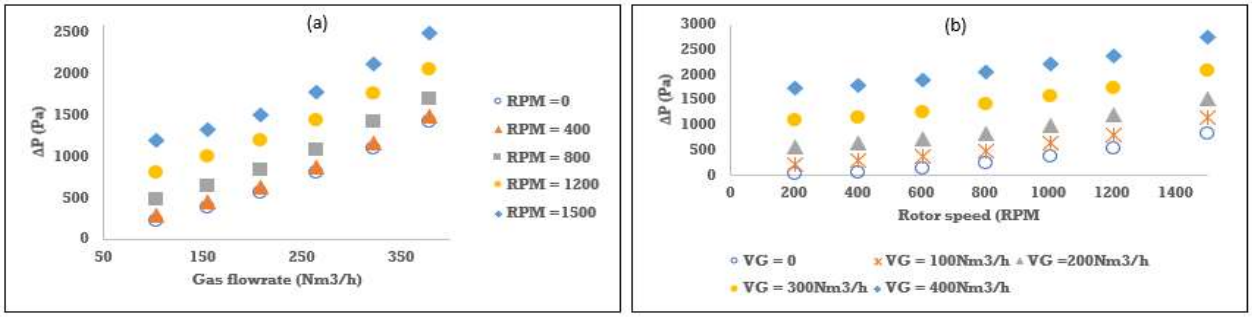

Figure 3: Dry bed pressure drop (a) effect of rotation speed (b) effect of gas flowrate

By comparing Figures 4(a) and (b), it can be seen that based on the sensitivity analysis mentioned above, the gas flow influences the dry pressure drop of the RPB more than the rotational speed. It can be deduced from figures 4(a) and (b) that the range of dry pressure drops (20-2800Pa) in this work was comparable to the range obtained by (Liu et al., 2018) for the same range of rotation speed and comparable gas loads. The result is also comparable to that of (Neumann, Hunold, Skiborowski, et al., 2017) of 20-750Pa for similar rotation speed, RPB, and packing characteristics but using a lower gas flow rate of 15-60m^3/h. For the irrigated bed, Figures 5(a) and (b), as well as Figure 6(a), showed that the trend of the pressure drop variation was almost the same as that of the dry bed, with the pressure increasing with an increase in rotational speed and with the gas flow. (W. Zhang et al., 2020) identified the wetting of the packing surface, which affects the frictional pressure drop, and the blockage of the packing pores by the liquid to the passage of gas as the two principal contributors to the rise in pressure drop in wet RPBs. Figure 6(b) indicates the lower effect of liquid flow rate on the overall pressure drop in RPBs. For example, for a gas flow of 350Nm^3/h, the 50% increase in liquid flow rate from 0.3 to 0.6m^3/h produces small changes in the pressure drop with the increase in the speed of rotation, showing that the effect of the gas flow in the RPB is more than that of the liquid flows. This phenomenon is more visible when we represent this at constant rotational speeds with a variation of the gas flow (Figure 5a) or a variation of the liquid flow (Figure 5(b)). These results confirm the trends described by the reports of (Groß et al., 2018; Neumann, Hunold, Groß, et al., 2017). Additionally, in terms of liquid loading loads and gas capacities, it can be deduced that the ranges of the wet pressure drops in Figures 6(a) and (b) are comparable to the findings of (Liu et al., 2018).

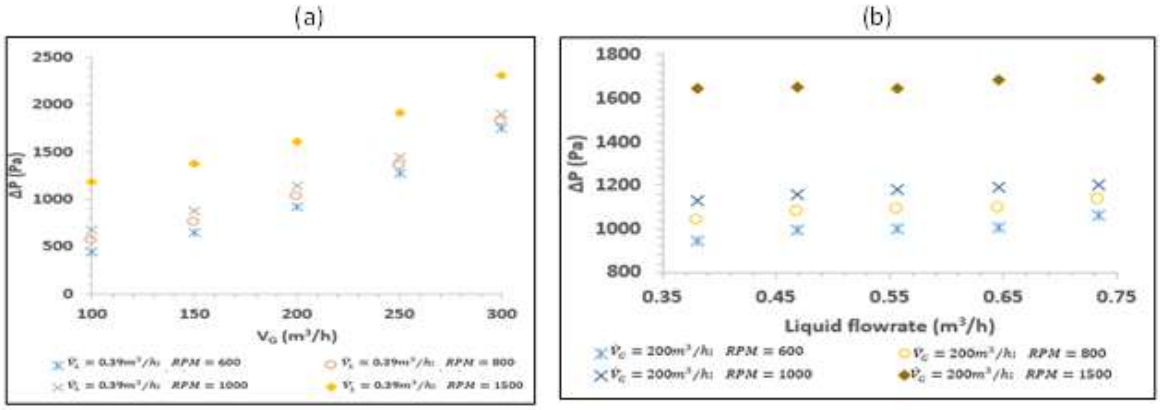

Figure 4 (a)Dry pressure drop increases with increased rotor speed. (b) Average increase in pressure drop per unit increase in gas flow rate.

Figure 4 (a) shows that the flooding data follows a typical RPB equipped with a vertical axis pressure drop variation curve with rotation speed at constant gas and liquid flow rates, as highlighted by (Neumann, Hunold, Groß, et al., 2017). A lowering of centrifugal pressure drop is obtained at a decrease from the maximum rotation speeds. At the same time, liquid accumulation in the eye causes only slight increases in frictional pressure drop. Further decrease in the rotation speed will cause an accumulation of liquid in the eye of the rotor, which leads to an increase in the frictional pressure drop and a sharp increase in the total pressure drop.

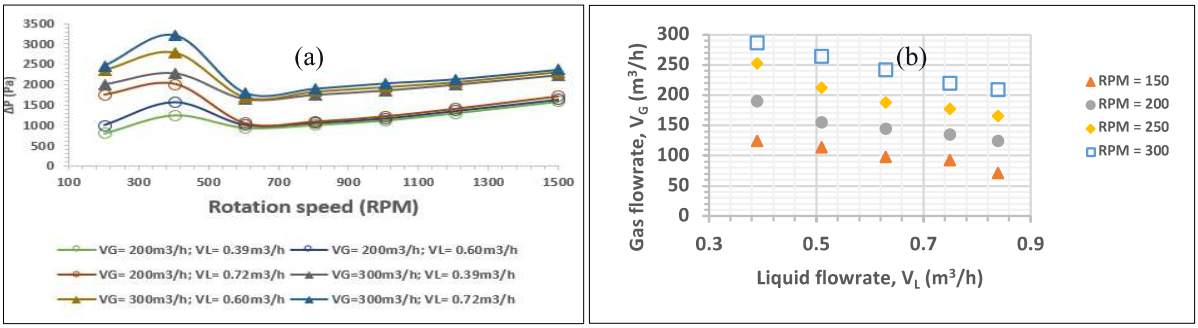

Figure 5 (a) Effect of rotation speed at constant gas and liquid flow rates (b) upper operating points.

As the rotation speed is further decreased, rapid ejection of liquid from the eye of the rotor to the gas outlet is obtained due to the acceleration of the liquid droplets. The pressure drop increases significantly, and the presence of water is visually observable in the rotor eye. Figure 6(b) shows the upper operating limits of the system investigated. At a constant rotation speed, the gas flow rate at which the ejection of liquid droplets was observed and decreased with an increased liquid flow rate. Regular operation of the RPB without liquid ejection and possible high-pressure drops, which increase power consumption, is obtained by operating the RPB below the indicated points. The operating limit at a given condition can be improved by increasing the rotation speed from the given point. Based on a range of liquid loads and the gas capacity factor at the inner radius of the RPB, the trends and ranges of these operating limits are comparable to the results of (Groß et al., 2018).

4. CONCLUSIONS

This paper focused on furthering the understanding of the upper operating limits of RPBs as an essential aspect of its design, modeling, scale-up, and use for the intensification of mass transfer processes. The gas pressure drop of a pilot-scale RPB equipped with stainless steel wire mesh packing for an air-water system using a twin-nozzle liquid distributor was explored. A robust approach to determine RPB operating limits based on quantifying the volume of liquid ejected from the eye of the rotor was explored. The operating limits for RPBs are influenced mainly by the three operational parameters: gas flow rate, liquid flow rate, and rotational speed in that order.

ACKNOWLEDGMENT

This work was conducted under support funding from the Overseas Scholarship Scheme (OSS) of the Petroleum Technology Development Fund (PTDF), Nigeria (Grant Number: PTDF/ED/OSS/PHD/UG/1543/19).

REFERENCES

Adekola L., Meihong W., Peter S, O. O. (2012). Demonstrating full-scale post-combustion CO2 capture for coal-fired power plants through dynamic modelling and simulation. *Fuel*, *101*, 115–128.

Burns, J. R., Jamil, J. N., & Ramshaw, C. (2000). Process intensification: Operating characteristics of rotating packed beds - determination of liquid hold-up for a high-voidage structured packing. *Chemical Engineering Science*, *55*(13), 2401–2415. https://doi.org/10.1016/S0009-2509(99)00520-5

Burns, J. R., & Ramshaw, C. (1996). Process intensification: Visual study of liquid maldistribution in rotating packed beds. *Chemical Engineering Science*, *51*(8), 1347–1352. https://doi.org/10.1016/0009-2509(95)00367-3

Chen, Y. S., Lin, F. Y., Lin, C. C., Tai, C. Y. Der, & Liu, H. S. (2006). Packing characteristics for mass transfer in a rotating packed bed. *Industrial and Engineering Chemistry Research*, *45*(20), 6846–6853. https://doi.org/10.1021/ie060399l

Cheng, H. H., & Tan, C. S. (2011). Removal of CO2 from indoor air by alkanolamine in a rotating packed bed. *Separation and Purification Technology*, *82*(1), 156–166. https://doi.org/10.1016/j.seppur.2011.09.004

Groß, K., Neumann, K., Skiborowski, M., & Górak, A. (2018). Analysing the operating limits in high gravity equipment. *Chemical Engineering Transactions*, *69*, 661–666. https://doi.org/10.3303/CET1869111

Hendry, J. R., Lee, J. G. M., & Attidekou, P. S. (2020). Pressure drop and flooding in rotating packed beds. *Chemical Engineering and Processing - Process Intensification*, *151*(March), 107908. https://doi.org/10.1016/j.cep.2020.107908

Hilpert, M., & Repke, J. U. (2021). Experimental Investigation and Correlation of Liquid-Side Mass Transfer in Pilot-Scale Rotating Packed Beds. *Industrial and Engineering Chemistry Research*, *60*(14), 5251–5263. https://doi.org/10.1021/acs.iecr.1c00440

Jiao, W. Z., Liu, Y. Z., & Qi, G. S. (2010). Gas pressure drop and mass transfer characteristics in a cross-flow rotating packed bed with porous plate packing. *Industrial and Engineering Chemistry Research*, *49*(8), 3732–3740. https://doi.org/10.1021/ie9009777

Liu, X., Jing, M., Chen, S., & Du, L. (2018). Experimental study of gas pressure drop in rotating packed bed with rotational-stationary packing. *Canadian Journal of Chemical Engineering*, *96*(2), 590–596. https://doi.org/10.1002/cjce.22936

Lockett, M. J. (1995). Flooding of rotating structured packing and its application to conventional packed columns. *Chem. Eng. Res. Des.*, *73*, 379–384.

Neumann, K., Gladyszewski, K., Groß, K., Qammar, H., Wenzel, D., Górak, A., & Skiborowski, M. (2018). A guide on the industrial application of rotating packed beds. *Chemical Engineering Research and Design*, *134*, 443–462. https://doi.org/10.1016/j.cherd.2018.04.024

Neumann, K., Hunold, S., Groß, K., & Górak, A. (2017a). Experimental investigations on the upper operating limit in rotating packed beds. *Chemical Engineering and Processing: Process Intensification*, *121*(August), 240–247. https://doi.org/10.1016/j.cep.2017.09.003

Neumann, K., Hunold, S., Skiborowski, M., & Górak, A. (2017b). Dry Pressure Drop in Rotating Packed Beds - Systematic Experimental Studies. *Industrial and Engineering Chemistry Research*, *56*(43), 12395–12405. https://doi.org/10.1021/acs.iecr.7b03203

Pan, S. Y., Wang, P., Chen, Q., Jiang, W., Chu, Y. H., & Chiang, P. C. (2017). Development of high-gravity technology for removing particulate and gaseous pollutant emissions: Principles and applications. *Journal of Cleaner Production*, *149*, 540–556. https://doi.org/10.1016/j.jclepro.2017.02.108

Pyka, T., Koop, J., Held, C., & Schembecker, G. (2022). Dry Pressure Drop in a Two-Rotor Rotating Packed Bed. *Industrial & Engineering Chemistry Research*. https://doi.org/10.1021/acs.iecr.2c02500

Singh, S. P., Counce, R. M., Wilson, J. H., Villiers-Fisher, J. F., Jennings, H. L., Lucero, A. J., Reed, G. D., Ashworth, R. A., & Elliott, M. G. (1992). Removal of Volatile Organic Compounds from Groundwater Using a Rotary Air Stripper. *Industrial and Engineering Chemistry Research*, *31*(2), 574–580. https://doi.org/10.1021/ie00002a019

Xie, P. (2019). *Hydrodynamics and Mass Transfer of Rotating Packed Beds for CO 2 Capture*. *February*.

Yuan, Z.-G., Wang, Y.-X., Liu, Y.-Z., Wang, D., Jiao, W.-Z., & Liang, P.-F. (2022). Research and development of advanced structured packing in a rotating packed bed. *Chinese Journal of Chemical Engineering*, *49*, 178–186. https://doi.org/10.1016/j.cjche.2021.12.023

Zhang, L. L., Wang, J. X., Xiang, Y., Zeng, X. F., & Chen, J. F. (2011). Absorption of carbon dioxide with ionic liquid in a rotating packed bed contactor: Mass transfer study. *Industrial and Engineering Chemistry Research*, *50*(11), 6957–6964. https://doi.org/10.1021/ie1025979

Zhang, W., Xie, P., Li, Y., Teng, L., & Zhu, J. (2020). Hydrodynamic characteristics and mass transfer performance of rotating packed bed for CO2 removal by chemical absorption: A review. *Journal of Natural Gas Science and Engineering*, *79*(March), 103373. https://doi.org/10.1016/j.jngse.2020.103373